JOURNAL OF GUIDANCE, CONTROL, AND DYNAMICS
Vol. 23, No. 6, November–December 2000

Adaptive Output Feedback Control of a Nonlinear Aeroelastic Structure

WenHong Xing* and Sahjendra N. Singh†
University of Nevada, Las Vegas, Nevada 89154-4026

Based on a backstepping design technique, a new adaptive controller for the control of an aeroelastic system using output feedback is derived. The chosen dynamic model describes the nonlinear plunge and pitch motion of a wing. The parameters of the system are assumed to be completely unknown, and only the plunge displacement and the pitch angle measurements are used for the synthesis of the controller. A canonical state variable representation of the system is derived, and filters are designed to obtain the estimates of the derivatives of the pitch angle and the plunge displacement. Then adaptive control laws for the trajectory control of the pitch angle and the plunge displacement are derived. In the closed-loop system the state vector asymptotically converges to the origin. Simulation results are presented, which show that regulation of the state vector to the equilibrium state and trajectory following are accomplished using a single control surface in spite of the uncertainty in the aerodynamic and structural parameters.

Nomenclature

a	=	nondimensionalized distance from the midchord to the elastic axis
b_s	=	semichord of the wing
c_h	=	structural damping coefficient in plunge caused by viscous damping
c_i, L, L_i, d_i, Γ	=	design parameters
c_α	=	structural damping coefficient in pitch caused by viscous damping
h	=	plunge displacement
I_α	=	mass moment of inertia of the wing about the elastic axis
k_h	=	structural spring constant in plunge
k_α	=	structural spring constant in pitch
m	=	mass
q, x	=	states of the aeroelastic system
U	=	freestream velocity
v_i, s_i	=	components of Ω
x_α	=	nondimensionalized distance measured from the elastic axis to the center of mass
α	=	pitch angle
β	=	flap deflection
θ, ρ; $\hat{\theta}$, $\hat{\rho}$	=	parameters; estimate of parameters
ξ, Ω	=	filter states
ρ	=	density of air

Introduction

AEROELASTIC systems exhibit a variety of phenomena including instability, limit cycle, and even chaotic vibration.[1–3] Active control of aeroelastic instability is an important problem. Several researchers have analyzed the stability properties of aeroelastic systems and designed controllers for flutter suppression.[4–10] Mukhopadhyay et al.[5] and Gangsass et al.[6] developed methods for obtaining lower-order models and designed controllers. Karpel[7] used pole placement technique to design controllers for flutter suppression and gust alleviation. Horikawa and Dowell[9] performed flutter analysis using root-locus plots. Piezoelectric actuation has been considered for flutter control in Refs. 10 and 11. In these studies linear control theory has been used for the design of controllers. Digital adaptive control of a linear autoregressive moving average aeroservoelastic model has been considered by Friedmann et al.[12] At the NASA Langley Research Center a benchmark active control technique wind-tunnel model has been designed, and control algorithms for flutter suppression have been developed.[13] Because the linear design is often not adequate, researchers have developed control systems for nonlinear aeroelastic models.[14–16] Although nonlinearities arising from control saturation, free play, hysteresis, and stability derivatives are encountered in aeroelastic systems, nonlinear structural stiffness can play a dominant role in causing the onset of flutter.

Recently, an aeroelastic apparatus has been developed, and tests have been performed in a wind tunnel to examine the effect of nonlinear structural stiffness.[16] In a series of interesting papers, Ko et al.[17] and Ko and Strganac[18] have designed control systems for this aeroelastic system using a feedback linearizing technique and an adaptive control strategy. In a study by Block and Strganac,[19] the unsteady aerodynamics are modeled with an approximation to Theodorsen's theory, and linear control laws are derived for the active control of the aeroelastic model described in Ref. 16. A variable structure adaptive control of a prototypical aeroelastic wing has been also considered in Ref. 20. Because the aerodynamic and structural parameters are not known precisely, the adaptive controllers designed in Refs. 18 and 20 are useful. However, the adaptive design in Ref. 18 requires complete knowledge of the state variables and uses two control surfaces for state regulation. Although the variable structure adaptive controller of Ref. 20 uses only output feedback, the assumption is made that the bounds on uncertain parameters are known for the control law derivation. Furthermore, this controller uses a high-gain feedback, which often leads to control saturation and can cause instability. Thus it is important to develop control systems for the active control of aeroelastic systems using output feedback in the presence of parameter uncertainty.

The contribution of this paper lies in the design of a new adaptive control law for the control of a nonlinear aeroelastic system using only output feedback. A single trailing-edge control surface is used for the control of the pitch and plunge motion of the system. For the synthesis of the controller, the assumption is made that only pitch angle and plunge displacement are measured. A canonical state variable representation of the system is derived for the reconstruction of the state variables. Based on the new state variable form of the aeroelastic system, filters are designed, and an estimate of states are constructed using a linear combination of the states of the filters. Then based on a backstepping design technique of Kanellakopoulos et al.[21] and Krstic et al.,[22] adaptive control laws for the control of the pitch angle and the plunge displacement are

Received 21 January 1999; revision received 9 September 1999; accepted for publication 10 September 1999.

*Graduate Student, Electrical and Computer Engineering Department.
†Professor, Electrical and Computer Engineering Deptartment. Associate Fellow AIAA.

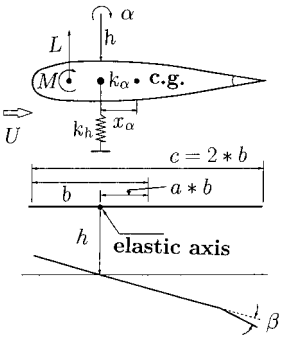

Fig. 1 Aeroelastic model.

derived. In the closed-loop system the state vector of the aeroelastic system asymptotically converges to the origin. Simulation results are presented to show the adaptive state regulation capability of the control systems.

Aeroelastic Model and Control Problem

The prototypical aeroelastic wing section is shown in Fig. 1. The governing equations of motion are provided in Ref. 17, which are given by

$$\begin{bmatrix} m & mx_\alpha b_s \\ mx_\alpha b_s & I_\alpha \end{bmatrix}\begin{bmatrix} \ddot{h} \\ \ddot{\alpha} \end{bmatrix} + \begin{bmatrix} c_h & 0 \\ 0 & c_\alpha \end{bmatrix}\begin{bmatrix} \dot{h} \\ \dot{\alpha} \end{bmatrix} + \begin{bmatrix} k_h & 0 \\ 0 & k_\alpha(\alpha) \end{bmatrix}\begin{bmatrix} h \\ \alpha \end{bmatrix} = \begin{bmatrix} -L \\ M \end{bmatrix} \tag{1}$$

In Eq. (1) M and L are the aerodynamic lift and moment. The assumption is made that the quasi-steady aerodynamic force and moment are of the form

$$L = \rho U^2 b_s c_{l_\alpha}\left[\alpha + (\dot{h}/U) + \left(\tfrac{1}{2} - a\right)b_s(\dot{\alpha}/U)\right] + \rho U^2 b_s c_{l_\beta}\beta$$

$$M = \rho U^2 b_s^2 c_{m_\alpha}\left[\alpha + (\dot{h}/U) + \left(\tfrac{1}{2} - a\right)b_s(\dot{\alpha}/U)\right] + \rho U^2 b_s^2 c_{m_\beta}\beta \tag{2}$$

where c_{l_α} and c_{m_α} are the lift and moment coefficients per angle of attack and c_{l_β} and c_{m_β} are lift and moment coefficients per control surface deflection. Although other forms of nonlinear spring stiffness associated with the pitch motion can be considered, for purposes of illutration the function $k_\alpha(\alpha)$ is considered as a polynomial nonlinearity given by

$$k_\alpha(\alpha) = 2.82(1 - 22.1\alpha + 1315.5\alpha^2 - 8580\alpha^3 + 17{,}289.7\alpha^4) \tag{3}$$

Defining the state vector $q = (\alpha, h, \dot{\alpha}, \dot{h})^T$, one obtains a state variable representation of Eq. (1) in the form

$$\dot{q} = \begin{bmatrix} 0_{2\times 2} & I_{2\times 2} \\ M_1 & M_2 \end{bmatrix} q + \begin{bmatrix} 0_{2\times 1} \\ g \end{bmatrix} k_{n_\alpha}(\alpha) + \begin{bmatrix} 0_{2\times 1} \\ b \end{bmatrix}\beta \tag{4}$$

where $\alpha k_\alpha = \alpha k_{\alpha_0} + k_{n_\alpha}$, $k_{n_\alpha} = k_{\alpha_1}\alpha^2 + k_{\alpha_2}\alpha^3 + k_{\alpha_3}\alpha^4 + k_{\alpha_4}\alpha^5$, $b = (b_1, b_2)^T$, $g = (g_1, g_2)^T$, 0 and I denote null and identity matrices of appropriate dimensions, and

$$M_1 = \begin{bmatrix} -\left(k_4 U^2 + md^{-1}k_{\alpha_0}\right) & -k_3 \\ -\left(k_2 U^2 - mx_\alpha b_s d^{-1}k_{\alpha_0}\right) & -k_1 \end{bmatrix}$$

$$M_2 = \begin{bmatrix} -c_{41} & -c_{31} \\ -c_{21} & -c_{11} \end{bmatrix}$$

The expression for the parameters k_i, d, c_{ij}, g_i, and b_i are given in Appendix A. The assumption is made that only signals α and h are measured.

Consider a reference trajectory y_r that represents either a prescribed pitch angle trajectory α_r for pitch angle control or a plunge displacement trajectory h_r for the plunge motion control. Appropriate reference trajectories are generated by a second-order command generator. We are interested in deriving output feedback adaptive control systems so that α tracks α_r or h tracks h_r asymptotically, and in the closed-loop system the state vector $(h, \alpha, \dot{h}, \dot{\alpha})^T$ converges to zero as $t \to \infty$.

Canonical System and State Estimation

Because $\dot{\alpha}$ and $\dot{h}$ are not measured, it is essential to obtain an estimate of these variables so that control synthesis can be accomplished. To obtain a state estimator, a representation of the system in a canonical form is obtained, which is useful in designing certain filters. Then a linear combination of filter states provides an estimate of the state vector.

Consider a state transformation $x = Tq$, where

$$T = \begin{bmatrix} I_{2\times 2} & 0_{2\times 2} \\ -M_2 & I_{2\times 2} \end{bmatrix} \tag{5}$$

Then it is easily seen that a new state variable representation of Eq. (1) is given by

$$\dot{x} = \begin{bmatrix} M_2 & I_{2\times 2} \\ M_1 & 0_{2\times 2} \end{bmatrix} x + \begin{bmatrix} 0_{2\times 1} \\ g \end{bmatrix} k_{n_\alpha}(\alpha) + \begin{bmatrix} 0_{2\times 1} \\ b \end{bmatrix}\beta \tag{6}$$

where $x = (x_1, x_2, x_3, x_4)^T$, $x_1 = \alpha$, and $x_2 = h$. Define

$$\begin{pmatrix} M_2 \\ M_1 \end{pmatrix}\begin{pmatrix} \alpha \\ h \end{pmatrix} + \begin{pmatrix} 0 \\ g \end{pmatrix} k_{n_\alpha}(\alpha) + \begin{pmatrix} 0 \\ b \end{pmatrix}\beta \doteq F^T(\alpha, h, \beta)\theta \tag{7}$$

where $\theta = [b^T, M_{2(1)}, M_{2(2)}, M_{1(1)}, M_{1(2)}, g_1 p_\alpha, g_2 p_\alpha]^T$, the superscript T denotes matrix transposition, $M_{i(k)}$ denotes the kth row of M_i, $p_\alpha = (k_{\alpha_1}, k_{\alpha_2}, k_{\alpha_3}, k_{\alpha_4})$, and the 4×18 matrix F^T is

$$F^T = \left(\beta e_3, \beta e_4, \alpha e_1, h e_1, \alpha e_2, h e_2, \alpha e_3, h e_3, \alpha e_4, h e_4, \alpha^2 e_3, \right.$$
$$\left. \alpha^3 e_3, \alpha^4 e_3, \alpha^5 e_3, \alpha^2 e_4, \alpha^3 e_4, \alpha^4 e_4, \alpha^5 e_4\right) \tag{8}$$

Here e_k denotes a vector of appropriate dimension whose kth element is one, and the remaining elements are zero.

Using the definition of matrix F, Eq. (6) can be written as

$$\dot{x} = Ax + L[\alpha, h]^T + F^T(\alpha, h, \beta)\theta \tag{9}$$

where $L = (L_1^T, L_2^T)^T$,

$$L_i = \begin{pmatrix} L_{i1} & 0 \\ 0 & L_{i2} \end{pmatrix}, \qquad A = \begin{bmatrix} -L_1 & I_{2\times 2} \\ -L_2 & 0_{2\times 2} \end{bmatrix}$$

The matrices L_1, L_2 are chosen so that A is a stable matrix. Equation (9) is a canonical representation of system Eq. (1) in which A is in a special from, the regressor matrix F is a function of the measured variables and the input β, and all unknown parameters of the system are included in the vector θ. Based on Eq. (9), certain filters are designed.

In view of Eq. (9), following Ref. 22, filters are given by

$$\dot{\xi} = A\xi + L[\alpha, h]^T, \qquad \dot{\Omega}^T = A\Omega^T + F^T(\alpha, h, \beta) \tag{10}$$

where $\xi \in R^4$ and $\Omega^T \in R^{4\times 18}$. Define a state estimate as

$$\hat{x} = \xi + \Omega^T\theta \tag{11}$$

and let the state error be $\tilde{x} = (x - \hat{x})$. Using Eqs. (9–11), the error $\tilde{x}$ is governed by

$$\dot{\tilde{x}} = A\tilde{x} \tag{12}$$

Because A is a Hurwitz matrix, $\tilde{x}(t) \to 0$ as $t \to \infty$, and, therefore, $\hat{x}(t)$ asymptotically converges to $x(t)$. Of course, θ is not known, and Eq. (11) cannot be used to construct $\hat{x}(t)$. However, Eq. (11) is useful in the derivation of an adaptive control law.

For simplicity in synthesis and in view of the special form of the matrix F, one can reduce the dimension of the Ω filter. Define

$$\Omega^T = [v_1, v_0, s_1, s_2, \ldots, s_{16}] \doteq [v_1, v_0, S] \tag{13}$$

where each column of Ω^T is a 4×1 vector. Because of the special structure of F^T in Eq. (8), it follows from Eq. (10) that v_i and s_i satisfy

$$\dot{v}_1 = Av_1 + e_3\beta, \qquad \dot{v}_0 = Av_0 + e_4\beta$$

$$\dot{s}_1 = As_1 + e_1\alpha, \qquad \dot{s}_2 = As_2 + e_1h, \qquad \dot{s}_3 = As_3 + e_2\alpha$$

$$\dot{s}_4 = As_4 + e_2h, \qquad \dot{s}_5 = As_5 + e_3\alpha, \qquad \dot{s}_6 = As_6 + e_3h$$

$$\dot{s}_7 = As_7 + e_4\alpha, \qquad \dot{s}_8 = As_8 + e_4h, \qquad \dot{s}_9 = As_9 + e_3\alpha^2$$

$$\dot{s}_{10} = As_{10} + e_3\alpha^3, \quad \dot{s}_{11} = As_{11} + e_3\alpha^4, \quad \dot{s}_{12} = As_{12} + e_3\alpha^5$$

$$\dot{s}_{13} = As_{13} + e_4\alpha^2, \qquad \dot{s}_{14} = As_{14} + e_4\alpha^3$$

$$\dot{s}_{15} = As_{15} + e_4\alpha^4, \qquad \dot{s}_{16} = As_{16} + e_4\alpha^5 \tag{14}$$

Noting that $e_2 = Ae_4$ and $e_1 = Ae_3$, in view of Eq. (14) one finds that

$$s_1 = As_5, \qquad s_2 = As_6, \qquad s_3 = As_7, \qquad s_4 = As_8 \tag{15}$$

That is, s_i $(i = 1, \ldots, 4)$ can be simply obtained by using Eq. (15) for synthesis. Thus for synthesis one needs filters of dimension 60, which is a large number. However, implementation of these filters is easy because they have simple transfer matrices. However, for the purpose of analysis Eq. (14) will be used.

Adaptive Control Laws

First the derivation of the control law for the trajectory control of the pitch angle is considered.

Pitch Angle Control

Let $y_r = \alpha_r$ be a smooth trajectory, which is to be tracked by α. In view of Eqs. (6) and (11), the derivative of the controlled output variable α is given by

$$\dot{\alpha} = x_3 + M_{2(1)}[\alpha, h]^T = \xi_3 + \Omega_{(3)}^T\theta + \tilde{x}_3 + M_{2(1)}[\alpha, h]^T \tag{16}$$

where $\Omega_{(k)}^T$, ξ_k, and $\tilde{x}_k$ denote kth rows of Ω^T, ξ_k, and $\tilde{x}_i$, respectively. Using the definitions of θ and Ω^T, Eq. (16) gives

$$\dot{\alpha} = b_1v_{13} + \xi_3 + \tilde{x}_3 + \bar{\omega}^T\theta \tag{17}$$

where $\bar{\omega}^T = [0, v_{03}, S_{(3)} + e_3^T\alpha + e_4^Th]$, $M_{2(1)} = (\theta_3, \theta_4)$, and v_{ik} and $S_{(k)}$ denote the kth rows of v_i and S, respectively. Because we are interested in the trajectory control of $y = \alpha$, consider the tracking error z_1 defined as

$$z_1 = y - y_r \tag{18}$$

Now the controller design is performed in two steps following a backstepping technique of Ref. 21.

Step 1

The derivative of z_1 is

$$\dot{z}_1 = b_1v_{13} + \xi_3 + \tilde{x}_3 + \bar{\omega}^T\theta - \dot{y}_r \tag{19}$$

Because v_{13} is treated as a virtual control for controlling z_1, define

$$z_2 = v_{13} - \hat{\rho}\dot{y}_r - \alpha_1 \tag{20}$$

where $\hat{\rho}$ is an estimate of $\rho = b_1^{-1}$ and α_1 is the stabilizing function yet to be chosen. Using Eq. (20) in Eq. (19) gives

$$\dot{z}_1 = \tilde{x}_3 + \xi_3 + b_1(z_2 + \alpha_1 + \hat{\rho}\dot{y}_r) + \bar{\omega}^T\theta - \dot{y}_r \tag{21}$$

The stabilizing function α_1 is chosen as

$$\alpha_1 = \hat{\rho}\bar{\alpha}_1, \qquad \bar{\alpha}_1 = -c_1z_1 - \xi_3 - \bar{\omega}^T\hat{\theta} - d_1z_1 \tag{22}$$

where c_i, $d_i > 0$ and $\hat{\theta}$ is an estimate of θ. Noting that $b_1\hat{\rho} = b_1(\rho - \tilde{\rho}) = 1 - b_1\tilde{\rho}$, it follows from Eqs. (21) and (22) that

$$\dot{z}_1 = b_1z_2 - b_1\tilde{\rho}\bar{\alpha}_1 + \bar{\omega}^T\tilde{\theta} - d_1z_1 + \tilde{x}_3 - b_1\tilde{\rho}\dot{y}_r - c_1z_1 \tag{23}$$

Now consider a Lyapunov function of the form

$$V_1 = d_1^{-1}\tilde{x}^TP\tilde{x} + \left(z_1^2 + |b_1|\gamma^{-1}\tilde{\rho}^2\right)\Big/2 \tag{24}$$

where $\gamma > 0$ and the positive definite symmetric matrix P satisfies the Lyapunov equation

$$PA + A^TP = -I_{4\times4} \tag{25}$$

Because A is a stable matrix, P is the unique solution of Eq. (25). The derivative of V_1 is given by

$$\dot{V}_1 = d_1^{-1}\left(\dot{\tilde{x}}^TP\tilde{x} + \tilde{x}^TP\dot{\tilde{x}}\right) + z_1\dot{z}_1 - |b_1|\gamma^{-1}\tilde{\rho}\dot{\hat{\rho}} \tag{26}$$

Substituting Eqs. (12), (23), and (25) into Eq. (26) gives

$$\dot{V}_1 = b_1z_1z_2 + \bar{\omega}^T\tilde{\theta}z_1 - c_1z_1^2 - |\tilde{x}|^2/d_1 - b_1\tilde{\rho}\bar{\alpha}_1z_1$$

$$- d_1z_1^2 + \tilde{x}_3z_1 - (\hat{\rho}|b_1|/\gamma)\tilde{\rho} - b_1\tilde{\rho}\dot{y}_rz_1 \tag{27}$$

where $|\cdot|$ denotes the Euclidean norm of a vector. Using Young's inequality [22], one has

$$\tilde{x}_3z_1 \le |\tilde{x}_3||z_1| \le d_1z_1^2 + \tilde{x}_3^2\Big/(4d_1) \le d_1z_1^2 + |\tilde{x}|^2\Big/(4d_1) \tag{28}$$

Using Eq. (28) in Eq. (27) gives

$$\dot{V}_1 \le b_1z_1z_2 + \bar{\omega}^T\tilde{\theta}z_1 - c_1z_1^2 - 3|\tilde{x}|^2/4d_1$$

$$+ z_1\tilde{\rho}[-b_1\bar{\alpha}_1 - b_1\dot{y}_r] - \dot{\hat{\rho}}|b_1|\tilde{\rho}/\gamma \tag{29}$$

Because $\tilde{\rho}$ is unknown, this can be eliminated from Eq. (29) by choosing an update law of the form

$$\dot{\hat{\rho}} = -\gamma\ \mathrm{sign}(b_1)[z_1(\bar{\alpha}_1 + \dot{y}_r)] \tag{30}$$

Now substituting the update law in Eq. (29) gives

$$\dot{V}_1 \le -c_1z_1^2 - (3/4d_1)|\tilde{x}|^2 + \bar{\omega}^T\tilde{\theta}z_1 + b_1z_1z_2 \tag{31}$$

The unknown θ-dependent term in Eq. (31) will be compensated in the second step.

Step 2

The derivative of z_2 is given by

$$\dot{z}_2 = \dot{v}_{13} - \dot{\hat{\rho}}\dot{y}_r - \hat{\rho}\ddot{y}_r - \dot{\alpha}_1 \tag{32}$$

Because α_1 is a function of $\hat{\rho}$, ξ_3, $S_{(3)}$, v_{03}, y_r, $\hat{\theta}$, x_1, x_2, its derivative is given by

$$\dot{\alpha}_1 = \frac{\partial\alpha_1}{\partial v_{03}}\dot{v}_{03} + \frac{\partial\alpha_1}{\partial\hat{\rho}}\dot{\hat{\rho}} + \frac{\partial\alpha_1}{\partial\xi_3}\dot{\xi}_3 + \frac{\partial\alpha_1}{\partial S_{(3)}}\dot{S}_{(3)}^T + \frac{\partial\alpha_1}{\partial y_r}\dot{y}_r + \frac{\partial\alpha_1}{\partial\hat{\theta}}\dot{\hat{\theta}}$$

$$+ \frac{\partial\alpha_1}{\partial x_1}\dot{x}_1 + \frac{\partial\alpha_1}{\partial x_2}\dot{x}_2 \doteq a_0 + \left(\frac{\partial\alpha_1}{\partial x_1}\right)\dot{x}_1 + \left(\frac{\partial\alpha_1}{\partial x_2}\right)\dot{x}_2 \tag{33}$$

where a_0 is obtained by comparing terms in Eq. (33). For the computation of a_0, the derivatives of various signals are substituted in Eq. (33), but $\dot{\hat{\theta}}$ is yet to be determined. Using Eqs. (6) and (11), the derivative of x_2 is given by

$$\dot{x}_2 = M_{2(2)}[\alpha, h]^T + x_4 = M_{2(2)}[\alpha, h]^T + \tilde{x}_4 + \xi_4 + \Omega_{(4)}^T\theta \tag{34}$$

Noting that $M_{2(1)} = [\theta_3, \theta_4]$ and $M_{2(2)} = [\theta_5, \theta_6]$, and adding and subtracting appropriate $\hat{\theta}$-dependent terms, and using Eqs. (16) and (34) in Eq. (33) gives

$$\dot{\alpha}_1 = a_0 + \left(\frac{\partial\alpha_1}{\partial x_1}\right)\left[\xi_3 + \Omega_{(3)}^T\theta + \tilde{x}_3 + \theta_3\alpha + \theta_4h\right]$$

$$+ \left(\frac{\partial\alpha_2}{\partial x_2}\right)\left[\xi_4 + \Omega_{(4)}^T\theta + \tilde{x}_4 + \theta_5\alpha + \theta_6h\right]$$

$$\doteq a_1 + a_2^T\tilde{x}_\alpha + a_3^T\tilde{\theta} \tag{35}$$

where

$$a_1 = a_0 + \frac{\partial \alpha_1}{\partial x_1}\left[\xi_3 + \Omega_{(3)}^T\hat{\theta} + \hat{\theta}_3\alpha + \hat{\theta}_4 h\right] + \frac{\partial \alpha_1}{\partial x_2}\left[\xi_4 + \Omega_{(4)}^T\hat{\theta} + \hat{\theta}_5\alpha + \hat{\theta}_6 h\right]$$

$$a_2^T = \left[\frac{\partial \alpha_1}{\partial x_1}, \frac{\partial \alpha_1}{\partial x_2}\right], \qquad \tilde{x}_\alpha = [\tilde{x}_3, \tilde{x}_4]^T$$

$$a_3^T = \frac{\partial \alpha_1}{\partial x_1}\left[\Omega_{(3)}^T + e_3^T\alpha + e_4^T h\right] + \frac{\partial \alpha_1}{\partial x_2}\left[\Omega_{(4)}^T + e_5^T\alpha + e_6^T h\right]$$

Substituting Eq. (35) into Eq. (32) gives

$$\dot{z}_2 = -L_{21}v_{11} + \beta - \dot{\hat{\rho}}\dot{y}_r - \hat{\rho}\ddot{y}_r - a_1 - a_2^T\tilde{x}_\alpha - a_3^T\tilde{\theta}$$

$$\doteq a^\star - a_2^T\tilde{x}_\alpha - a_3^T\tilde{\theta} + \beta \tag{36}$$

where $a^\star = -L_{21}v_{11} - \dot{\hat{\rho}}\dot{y}_r - \hat{\rho}\ddot{y}_r - a_1$. In view of Eq. (36), we choose control β as

$$\beta = -a^\star - c_2 z_2 - d_2|a_2|^2 z_2 - \hat{b}_1 z_1 \tag{37}$$

Consider a Lyapunov function

$$V_2 = V_1 + d_2^{-1}\tilde{x}^T P\tilde{x} + \left(z_2^2 + \tilde{\theta}^T\Gamma^{-1}\tilde{\theta}\right)/2 \tag{38}$$

where Γ is a positive definite symmetric matrix. In view of Eq. (25), the derivative of V_2 is given by

$$\dot{V}_2 = \dot{V}_1 - |\tilde{x}|^2/d_2 + z_2\dot{z}_2 - \tilde{\theta}^T\Gamma^{-1}\dot{\hat{\theta}} \tag{39}$$

Using Eq. (36) in Eq. (39) and noting that $b_1 = \theta_1$ gives

$$\dot{V}_2 \le -c_1 z_1^2 - 3|\tilde{x}|^2/4d_1 + \bar{\omega}^T\tilde{\theta}z_1 + (\hat{\theta}_1 + \tilde{\theta}_1)z_1 z_2 - c_2 z_2^2 - d_2 z_2^2|a_2|^2 - \hat{\theta}_1 z_1 z_2 - z_2 a_2^T\tilde{x}_\alpha - a_3^T\tilde{\theta}z_2 - \tilde{\theta}^T\Gamma^{-1}\dot{\hat{\theta}} - |\tilde{x}|^2/d_2 \tag{40}$$

Define

$$\tau = (\bar{\omega}z_1 + e_1 z_1 z_2 - a_3 z_2) \tag{41}$$

Using Young's inequality, one has

$$\left|z_2 a_2^T\tilde{x}_\alpha\right| \le |z_2||a_2||\tilde{x}_\alpha| \le d_2 z_2^2\left|a_2^2\right| + \left|\tilde{x}_\alpha^2\right|/4d_2 \tag{42}$$

Substituting Eqs. (41) and (42) into Eq. (40) and noting that $|\tilde{x}_\alpha|^2 \le |\tilde{x}^2|$, one has

$$\dot{V}_2 \le -c_1 z_1^2 - c_2 z_2^2 - \tfrac{3}{4}\left(d_1^{-1} + d_2^{-1}\right)|\tilde{x}|^2 + \tilde{\theta}^T(\tau - \Gamma^{-1}\dot{\hat{\theta}}) \tag{43}$$

Now one chooses the adaptation law for $\hat{\theta}$ as

$$\dot{\hat{\theta}} = \Gamma\tau \tag{44}$$

which yields

$$\dot{V}_2 \le -c_1 z_1^2 - c_2 z_2^2 - \tfrac{3}{4}\left(d_1^{-1} + d_2^{-1}\right)|\tilde{x}|^2 \tag{45}$$

Theorem 1: Consider the closed-loop system Eqs. (4), (30), (37), and (44). Suppose that y_r is a bounded and smooth trajectory converging to zero, and the zero dynamics of the system are stable. Then the solution of Eq. (1) beginning from any initial condition $q(0) \in R^4$ is such that the tracking error $(\alpha - \alpha_r)$ and h tend to be zero as $t \to \infty$. Furthermore, if $y_r = 0$, then the state vector $q(t)$ tends to the origin as $t \to \infty$.

Proof: A proof is given in Appendix B.

Zero dynamics describe the internal dynamics of the system when the output $y = \alpha$ is identically zero. For the control of α, Theorem 1 assumes that the zero dynamics are stable. The stability properties of zero dynamics have been extensively examined in Refs. 17, 18, and 20. Stability of the zero dynamics is essential even in the nonadaptive output trajectory control systems.

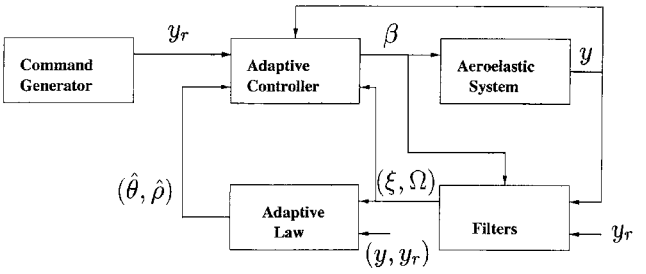

Fig. 2 Closed-loop system.

Adaptive Control of Plunge Motion

In the preceding section an adaptive control law for the trajectory control of α has been presented. Following a similar approach, one can derive a control law for the trajectory control of the plunge displacement. Define the tracking error

$$z_1 = h - h_r \tag{46}$$

Using Eq. (34), the differential equation for h is given by

$$\dot{h} = b_2 v_{04} + \xi_4 + \left[v_{14}, 0, S_{(4)}\right]\theta + \tilde{x}_4 + M_{(2)}[\alpha, h]^T \tag{47}$$

For controlling h, one treats v_{04} as the virtual control because in the derivative of v_{04} control input β appears. In this case $\rho = b_2^{-1}$ and

$$z_2 = v_{04} - \hat{\rho}\dot{h}_r - \alpha_1$$

Following the steps of the preceding section, one obtains a virtual control α_1 and the adaptation law for $\hat{\rho}$, which is an estimate of $\rho = b_2^{-1}$ in the first step of derivation, and the control law β and the update law for $\hat{\theta}$ is obtained in the second step. Because the control law for h control can be similarly derived, the details are not presented here. The complete closed-loop system is shown in Fig. 2.

Similar to α control, for the stability in the closed-loop system the assumption is made that the parameters of the aeroelastic system are such that the zero dynamics are stable. Unlike α control, the zero dynamics associated with the output h are nonlinear and exhibit complex dynamic behavior. In this case one has only local stability in the closed-loop system. Because a proof of stability can be established following the steps in the proof of Theorem 1, it is not presented here.

Simulation Results

In this section numerical results for the pitch angle control and plunge motion control are presented. The parameters of the system are given in Appendix A. Simulation is performed for different values of a and U. The transfer function of the command generator is chosen as

$$W_m = [\lambda^2/(s + \lambda)^2]$$

to obtain exponentially decaying command trajectories to zero where $\lambda > 0$. For the pitch angle control the initial conditions selected are $\alpha(0) = 5.75$ (deg), $h(0) = 0.01$ (m), $\dot{h}(0) = 0$, and $\dot{\alpha}(0) = 2$ (deg/s). The initial conditions of the command generator are set as $y_r(0) = 5.75$ (deg) and $\dot{y}_r(0) = 0$.

The initial conditions for the parameters are $\hat{b}_1(0) = -0.1$ and $\hat{b}_2(0) = -0.03$, and the remaining components of $\hat{\theta}$ and $\hat{\rho}$ have zero initial values. The initial states of the filters are set as $\Omega(0) = 0$ and $\xi(0) = 0$. The design parameters are selected as $\lambda = 1$, $c_1 = c_2 = d_3 = d_4 = 100$, $\gamma = 1$, $\Gamma = I_{18\times 18}$, $L_{11} = L_{12} = 20$, $L_{21} = L_{22} = 100$. These design parameters are chosen after several trials by observing simulated responses. The origin of the open-loop model (1) is unstable and undergoes persistent periodic oscillations (Readers may refer to Refs. 17–19 in which uncontrolled responses are provided).

Case 1: The closed-loop system Eq. (1) with the control law Eq. (37) and the update law Eqs. (30) and (44) for $a = -0.3$ and $U = 15$ m/s is simulated. For the chosen value of a and U, one has $b_1 = -0.282$ and $b_2 = -0.047$. Selected responses are shown

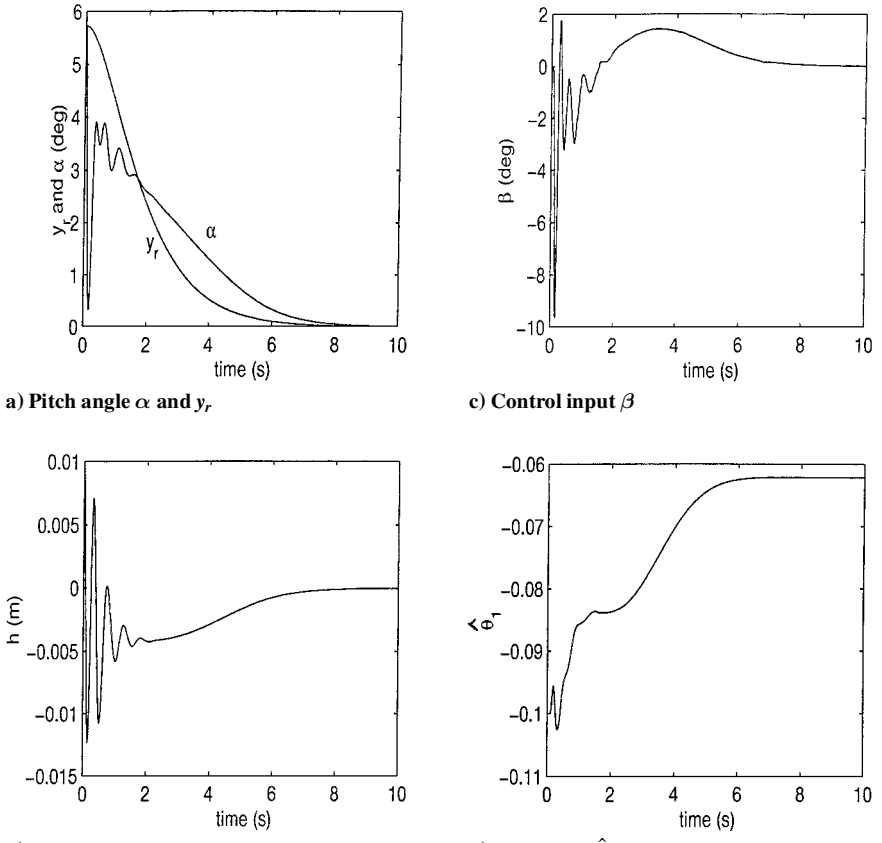

a) Pitch angle α and y_r c) Control input β

b) Plunge displacement h d) Parameter $\hat{\theta}_1$

Fig. 3 Pitch angle control $a = -0.3$ and $U = 15$ m/s.

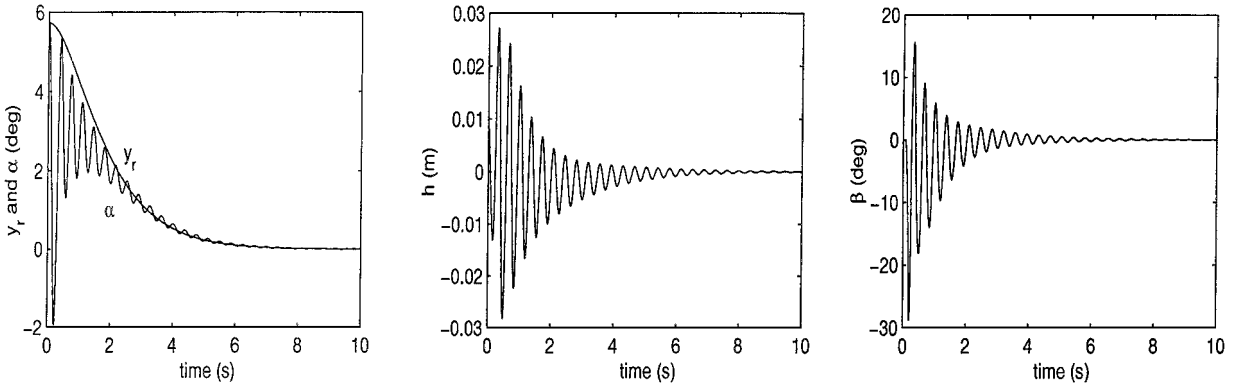

a) Pitch angle α and y_r b) Plunge displacement h c) Control input β

Fig. 4 Pitch angle control $a = -0.4$ and $U = 15$ m/s.

in Fig. 3. We observe that after an initial transient the pitch angle asymptotically tracks the command trajectory. The response time is of the order of 7–8 s. Only a small control magnitude (less than 10 deg) is required for control. Because for $a = -0.3$ and $U = 15$ m/s the zero dynamics are stable, the plunge displacement also converges to zero as predicted. Here only parameter $\hat{b}_1$ is shown in Fig. 3d, but it is found that all other components of $\hat{\theta}$ and $\hat{\rho}$ also converge to constant values.

Case 2: To examine the sensitivity of the controller with respect to parameter a, the closed-loop system for a different value of $a = -0.4$, but with the same value of $U = 15$ m/s, is simulated. We observe that although the pitch angle asymptotically tracks the command trajectory larger control magnitude (less than 30 deg) is required (Fig. 4). Moreover, larger plunge displacement is observed in this case. The response time is of the order of 6–7 s. In this case increase in control magnitude can be attributed to reduced degree of stability of the zero dynamics because as $a \rightarrow -0.55$ the poles of the zero dynamics move to the right in the complex plane (Ref. 16).

Case 3: The closed-loop system for $a = -0.4$ and $U = 20$ m/s is simulated. Selected responses are shown in Fig. 5. The response time of the same order as in case 2 is observed, but because of enhanced control effectiveness at higher air speed U, smaller control magnitude (about 18 deg) compared to case 2 is required. The plunge displacement and control input are somewhat similar to those of case 2, and, therefore, these plots are not shown here.

Case 4: Now simulation results for plunge motion control are presented. The parameters $c_i = d_i = 3000$ and $\Gamma = 300 I_{18 \times 18}$ are chosen. The initial conditions are $\alpha(0) = 5.75$ (deg), $h(0) = 0.01$ (m), and $\dot{\alpha}(0) = \dot{h}(0) = 0$. The remaining control parameters and initial conditions of case 1 are retained. The aeroelastic model for $a = -0.85$ and $U = 15$ m/s is considered for simulation. In this case $b_1 = 2.47$ and $b_2 = -0.21$. It is seen that h tracks y_r, and the pitch angle tends to zero (Fig. 6). Because the zero dynamics are nonlinear, we observe high-frequency oscillations in control β. The response time is of the order of 5–6 s. The maximum control magnitude is about 18 deg. Similar to case 1, all of the parameter estimates converge to constant values.

Case 5: Simulation for the aeroelastic model with $a = -0.88$ and $U = 15$ is performed. Selected responses are shown in Fig. 7. The state vector is regulated to zero, but compared to case 4 smoother response for h is obtained and transient in α decays relatively faster (in about 4 s). The control magnitude (about 17 deg) is also slightly smaller than case 4. For plunge control the degree of stability of the zero dynamics improves as the parameter $a \rightarrow -1$ (Ref. 16). For this reason the transient responses of h and α are better than those of case 4.

Case 6: To examine the sensitivity of the controller with respect to the air speed, a simulation is performed for the model with $U = 20$, but the remaining parameters of case 5 are retained. In this case one has $b_1 = 10$ and $b_2 = -0.8$. It is seen that h follows y_r and α is regulated to zero (Fig. 8). In this case at higher air speed, similar to case 3, smaller control magnitude (about 9.5 deg) compared to case 5 is required. The response time is of the order of 6–7 s.

Extensive simulation has been performed. Based on these results, by a suitable choice of parameters c_i, d_i, L, γ, Γ desirable responses

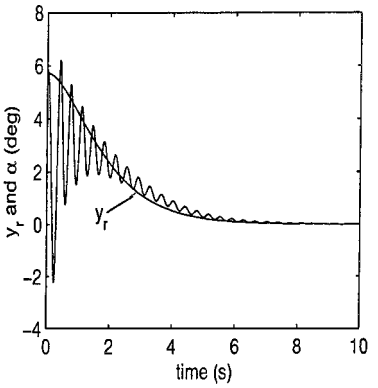

Fig. 5 Pitch angle control $a = -0.4$ and $U = 20$ m/s; pitch angle α and y_r.

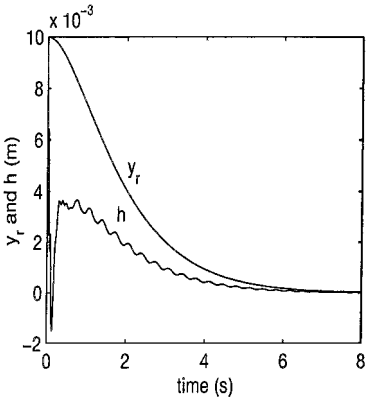

a) Plunge displacement h and y_r

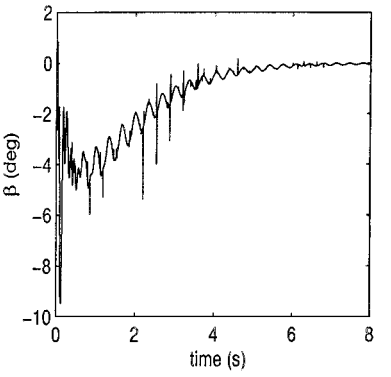

b) Control input β

Fig. 8 Plunge motion control $a = -0.88$ and $U = 20$ m/s.

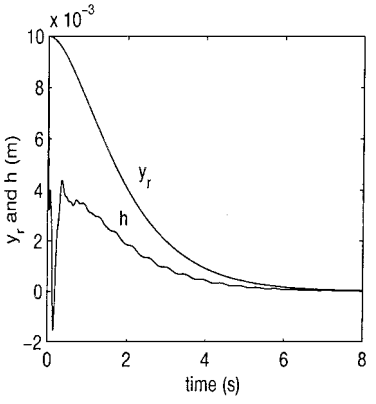

a) Plunge displacement h and y_r

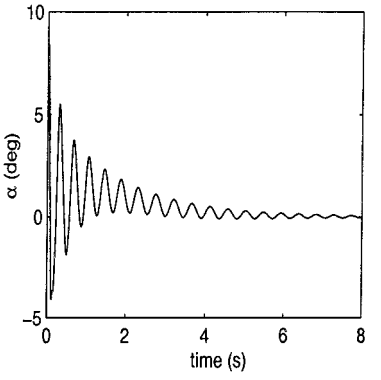

b) Pitch angle α

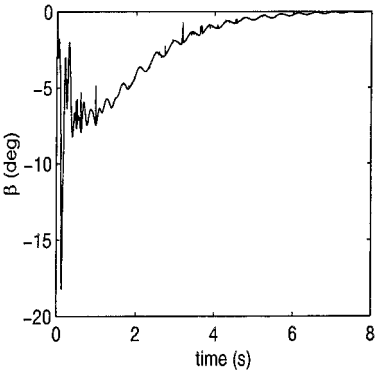

c) Control input β

Fig. 6 Plunge motion control $a = -0.85$ and $U = 15$ m/s.

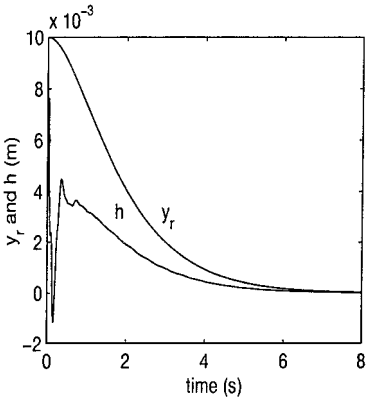

a) Plunge displacement h and y_r

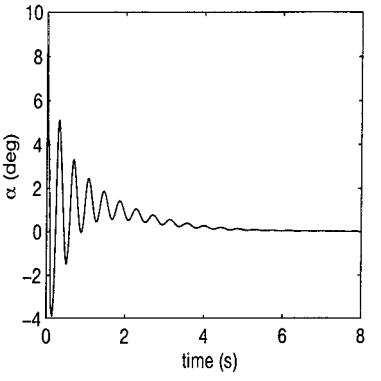

b) Pitch angle α

Fig. 7 Plunge motion control $a = -0.88$ and $U = 15$ m/s.

in the closed-loop system can be obtained. For smaller values of c_i, the control magnitude is reduced. Furthermore, the command trajectory y_r can be properly chosen to shape the transient responses.

Conclusions

In this paper, a new controller for the control of an aeroelastic system based on a backstepping design technique was presented. Adaptive control laws for the trajectory control of α and h were derived. For the derivation of the controller, a canonical representation of the aeroelastic model was obtained. Filters were designed to obtain the estimate of the state vector. In the closed-loop system asymptotic regulation of the state vector to the origin was accomplished. Simulation results were presented, which show that control of the pitch angle and the plunge displacement can be accomplished using output feedback in spite of the uncertainties in the system parameters. The adaptive controller has several design parameters that can be adjusted to obtain desirable response characteristics. Unlike a variable structure controller, adaptive design does not require high-gain feedback, and as such during the learning phase adaptive system does not provide good tracking performance if the initial parameter errors are large. However, the responses improve as the parameter learning and adaptation progresses.

Appendix A: System Parameters

$$b_s = 0.135\ \text{m}, \qquad k_h = 2844.4\ \text{N/m}, \qquad c_h = 27.43\ \text{Ns/m}$$

$$c_\alpha = 0.036\ \text{Ns}, \qquad \rho = 1.225\ \text{kg/m}^3, \qquad c_{l\alpha} = 6.28$$

$$c_{l\beta} = 3.358, \qquad c_{m\alpha} = (0.5 + a)c_{l\alpha}, \qquad c_{m\beta} = -0.635$$

$$m = 12.387\ \text{kg}, \qquad I_\alpha = 0.065\ \text{kgm}^2$$

$$x_\alpha = [0.0873 - (b_s + ab_s)]/b_s$$

System variables are given by

$$d = m\left(I_\alpha - mx_\alpha^2 b_s^2\right), \qquad k_1 = I_\alpha k_h/d$$

$$k_2 = \left(I_\alpha \rho b_s c_{l\alpha} + mx_\alpha b_s^3 \rho c_{m\alpha}\right)/d, \qquad k_3 = -mx_\alpha b_s k_h/d$$

$$k_4 = \left(-mx_\alpha b_s^2 \rho c_{l\alpha} - m\rho b_s^2 c_{m\alpha}\right)/d$$

$$c_{11} = \left[I_\alpha\left(c_h + \rho U b_s c_{l\alpha}\right) + mx_\alpha \rho U b_s^3 c_{m\alpha}\right]/d$$

$$c_{21} = \left[I_\alpha \rho U b_s^2 c_{l\alpha}\left(\tfrac{1}{2} - a\right) - mx_\alpha b_s c_\alpha + mx_\alpha \rho U b_s^4 c_{m\alpha}\left(\tfrac{1}{2} - a\right)\right]/d$$

$$c_{31} = \left(-mx_\alpha b_s c_h - mx_\alpha \rho U b_s^2 c_{l\alpha} - m\rho U b_s^2 c_{m\alpha}\right)/d$$

$$c_{41} = \left[mc_\alpha - mx_\alpha \rho U b_s^3 c_{l\alpha}\left(\tfrac{1}{2} - a\right) - m\rho U b_s^3 c_{m\alpha}\left(\tfrac{1}{2} - a\right)\right]/d$$

$$b_1 = U^2\left(mx_\alpha b_s^2 \rho c_{l\beta} + m\rho b_s^2 c_{m\beta}\right)/d$$

$$b_2 = U^2\left(-I_\alpha \rho b_s c_{l\beta} - mx_\alpha b_s^3 \rho c_{m\beta}\right)/d, \qquad g = \begin{bmatrix} -m/d \\ mx_a b_s/d \end{bmatrix}$$

Appendix B: Proof of Theorem 1

First it will be shown that all of the signals in the closed-loop system are bounded. V_2 is a positive definite function of z_1, z_2, $\tilde{\theta}$, $\tilde{\rho}$, $\tilde{x}$, and $\dot{V}_2$ is negative semidefinite. Thus, it follows that $(z_1, z_2, \tilde{\theta}, \tilde{\rho}, \tilde{x}) \in \mathcal{L}_\infty$, where $\mathcal{L}_\infty$ denotes the set of bounded functions. Because $z_1 \in \mathcal{L}_\infty$, one has $\alpha \in \mathcal{L}_\infty$.

Now the differential equations associated with the zero dynamics are derived. The output α has relative degree 2 because the control β appears in its second derivative. Thus the zero dynamics has dimension 2. Define

$$\eta = \begin{bmatrix} \eta_1 \\ \eta_2 \end{bmatrix} = \begin{bmatrix} b_2\alpha - b_1 h \\ b_2\dot{\alpha} - b_1\dot{h} \end{bmatrix} \tag{A1}$$

Then, using Eq. (1), it follows that η satisfies

$$\dot{\eta} = A_\eta \eta + (0, 1)^T f_\eta(\alpha, \dot{\alpha}) \tag{A2}$$

where

$$A_\eta = \begin{bmatrix} 0 & 1 \\ -a_{\eta 1} & -a_{\eta 2} \end{bmatrix}, \qquad c_{\eta i} = b_2 M_{i(1)} - b_1 M_{i(2)}, \qquad i = 1, 2$$

$$a_{\eta i} = c_{\eta i}\left(0, b_1^{-1}\right)^T, \qquad f_{n\eta} = (b_2, b_1) g k_{n\alpha}(\alpha)$$

$$f_\eta = (\alpha c_{\eta 1} + \dot{\alpha} c_{\eta 2})\left(1, b_2 b_1^{-1}\right)^T + f_{n\eta}$$

The zero dynamics are obtained when $\alpha = 0$ and $\dot{\alpha} = 0$, i.e., $f_\eta = 0$ in Eq. (A2). Thus, for the stability of the zero dynamics, A_η must be a Hurwitz matrix. Solving for η_1 from Eq. (A2), one obtains

$$\bar{\eta}_1(s) = \left[\frac{(c_{\eta 1} + sc_{\eta 2})\left(1, b_2 b_1^{-1}\right)^T}{H_\eta(s)}\right]\bar{\alpha}(s) + H_\eta^{-1}(s)\bar{f}_{n\eta}(\alpha) \tag{A3}$$

where in this Appendix s denotes the Laplace variable, functions with overbar denote Laplace transforms, and $H_\eta = s^2 + a_{\eta 2}s + a_{\eta 1}$. Because $(c_{\eta 1} + sc_{\eta 2})H_\eta^{-1}$ and H_η^{-1} are stable transfer functions and α is bounded, from Eq. (A3) it follows that η_1 is bounded. But $\eta_1 = b_2\alpha - b_1 h$, therefore, one has that $h \in \mathcal{L}_\infty$. Because $(\alpha, h) \in \mathcal{L}_\infty$, S and ξ are bounded. In view of the differential equations for v_1 and v_0 in Eq. (14), one has for $i = 0, 1$

$$\dot{v}_{i1} = -L_{11}v_{i1} + v_{i3}, \qquad \dot{v}_{i2} = -L_{12}v_{i2} + v_{i4}$$

$$\dot{v}_{i3} = -L_{21}v_{i1} + \delta_{i1}\beta, \qquad \dot{v}_{i4} = -L_{22}v_{i2} + \delta_{i0}\beta \tag{A4}$$

where $\delta_{ik} = 1$ if $i = k$, and it is zero otherwise. In view of Eq. (A4), it is easily seen that v_{01}, v_{03}, v_{12}, $v_{14} \in \mathcal{L}_\infty$, and this implies that $\bar{\omega}$ and α_1 are bounded. Because z_2 and α_1 are bounded, Eq. (20) implies that v_{13} is bounded. But in view of Eq. (A4), $v_{13} \in \mathcal{L}_\infty$ implies that $v_{11} \in \mathcal{L}_\infty$. This shows that $v_1 \in \mathcal{L}_\infty$ and $\Omega_{(3)}^T \in \mathcal{L}_\infty$, and in view of Eq. (16), $\dot{\alpha} \in \mathcal{L}_\infty$. Because α, $\dot{\alpha} \in \mathcal{L}_\infty$, using Eq. (A2) one concludes that $\eta \in \mathcal{L}_\infty$. Using Eq. (A1), now one has that $\dot{h} \in \mathcal{L}_\infty$. Using boundedness of $\dot{h}$, one concludes from Eq. (34) that $v_{02} \in \mathcal{L}_\infty$. Because $\dot{v}_{02} = -L_{12}v_{02} + v_{04}$, $v_{02} \in \mathcal{L}_\infty$. Thus, $v_0 \in \mathcal{L}_\infty$. This establishes the boundedness of all of the signals. Using the LaSalle–Yoshikawa theorem (Ref. 22, pp. 489–492), one has that $(z_1, z_2) \to 0$ as $t \to \infty$. Therefore, $\alpha \to 0$ as $t \to \infty$. In view of Eqs. (A3), η converges to zero, which according to Eq. (A1) implies that h converges to zero.

For the case when $y_r = 0$, according to the LaSalle invariance theorem (Ref. 22, p. 25) the state vector converges to the largest invariant set $\mathcal{V}_i$ contained in the set $\mathcal{V} = \{z_1 = 0, z_2 = 0, \tilde{x} = 0\}$. But in $\mathcal{V}_i$, $\dot{z}_1 = \dot{\alpha} = 0$. Now convergence of $(\dot{\alpha}, \eta_2)$ to zero implies convergence of $\dot{h}$ to zero. Therefore, $q(t)$ converges to zero. This completes the proof of Theorem 1.

References

[1] Fung, Y. C., *An Introduction to the Theory of Aeroelasticity*, Wiley, New York, 1955, pp. 207–215.

[2] Dowell, E. H., (ed.), *A Modern Course in Aeroelasticity*, Kluwer Academic, Norwell, MA, 1995, Chap. 1.

[3] Zhao, L. C., and Yang, Z. C., "Chaotic Motions of an Airfoil with Nonlinear Stiffness in Incompressible Flow," *Journal of Sound and Vibration*, Vol. 128, No. 2, 1990, pp. 245–254.

[4] Lyons, M. G., Vepa, R., McIntosh, I. E., and DeBra, D. B., "Control Law Synthesis and Sensor Design for Active Flutter Suppression," *Proceedings of the AIAA Guidance and Control Conference*, AIAA Paper 73-832, AIAA, New York, Aug. 1973.

[5] Mukhopadhyay, V., Newsom, J. R., and Abel, I., "Reduced-Order Optimal Feedback Control Law Synthesis for Flutter Suppression," *Journal of Guidance, Control, and Dynamics*, Vol. 5, No. 4, 1982, pp. 389–395.

[6] Gangsaas, D., Ly, U., and Norman, D. C., "Practical Gust Load Alleviation and Flutter Suppression Control Laws Based on LQG Methodology," AIAA Paper 81-0021, Jan. 1981.

[7] Karpel, M., "Design for Active Flutter Suppression and Gust Alleviation Using State-Space Aeroelastic Modeling," *Journal of Aircraft*, Vol. 19, No. 3, 1982, pp. 221–227.

[8] Edwards, J. W., Ashley, H., and Breakwell, J., "Unsteady Aerodynamic Modeling for Arbitrary Motions," *AIAA Journal*, Vol. 17, No. 4, 1979, pp. 365–374.

[9] Horikawa, H., and Dowell, E. H., "An Elementary Explanation of the Flutter Mechanism with Active Feedback Controls," *Journal of Aircraft*, Vol. 16, No. 4, 1979, pp. 225–232.

[10]Heeg, J., "Analytical and Experimental Investigation of Flutter Suppression by Piezoelectric Actuation," NASA TP 3241, Sept. 1993.

[11]Lazarus, K., Crawey, E., and Lin, C., "Fundamental Mechanisms of Aeroelastic Control with Control Surface and Strain Actuation," *Journal of Guidance, Control, and Dynamics*, Vol. 18, No. 1, 1995, pp. 10–17.

[12]Friedmann, P. P., Guillot, D., and Presente, E., "Adaptive Control of Aeroelastic Instabilities in Transonic Flow and Its Scaling," *Journal of Guidance, Control, and Dynamics*, Vol. 20, No. 6, 1997, pp. 1190–1199.

[13]Waszak, M. R., "Robust Multivariable Flutter Suppression for the Benchmark Active Control Technology (BACT) Wind-Tunnel Model," *11th Symposium on Structure Dynamics and Control*, Blacksburg, VA, May 1997.

[14]Tang, D. M., and Dowell, E. H., "Flutter and Stall Response of a Helicopter Blade with Structural Nonlinearity," *Journal of Aircraft*, Vol. 29, No. 5, 1990, pp. 953–960.

[15]Lee, B. H. K., and LeBlanc, P., "Flutter Analysis of a Two-Dimensional Airfoil with Cubic Nonlinear Restoring Force," National Aeronautical Establishment, Aeronautical Note 36, Canada National Research Council 25438, Ottawa, PQ, Canada, Feb. 1986.

[16]O'Neil, T., Gilliatt, H. C., and Strganac, T. W., "Investigations of Aeroelastic Response for a System with Continuous Structural Nonlinearities," AIAA Paper 96-1390, April 1996.

[17]Ko, J., Kurdila, A. J., and Strganac, T. W., "Nonlinear Control of a Prototypical Wing Section with Torsional Nonlinearity," *Journal of Guidance, Control, and Dynamics*, Vol. 20, No. 6, 1997, pp. 1181–1189.

[18]Ko, J., and Strganac, T. W., "Stability and Control of a Structurally Nonlinear Aeroelastic System," *Journal of Guidance, Control, and Dynamics*, Vol. 21, No. 5, 1998, pp. 718–725.

[19]Block, J., and Strganac, T. M., "Applied Active Control for a Nonlinear Aeroelastic Structure," *Journal of Guidance, Control, and Dynamics*, Vol. 21, No. 6, 1998, pp. 838–845.

[20]Zeng, Y., and Singh, S. N., "Output Feedback Variable Structure Adaptive Control of an Aeroelastic System," *Journal of Guidance, Control, and Dynamics*, Vol. 21, No. 6, 1998, pp. 830–837.

[21]Kanellakopoulos, I., and Kokotovic, P. V., and Morse, A. S., "Systematic Design of Adaptive Controller for Feedback Linearizable Systems," *IEEE Transaction on Automatic Control*, Vol. 36, No. 11, 1991, pp. 1241–1253.

[22]Krstic, M., Kanellakopoulos, I., and Kokotovic, P. V., *Nonlinear Adaptive Control Design*, Wiley, New York, 1995, pp. 24, 25, 327–346.